Available online at www.sciencedirect.com
ScienceDirect
Journal of the European Ceramic Society 28 (2008) 2275–2279
www.elsevier.com/locate/jeurceramsoc

Combustion synthesis of TiC_x–TiB_2 composites with hypoeutectic, eutectic and hypereutectic microstructures

Binglin Zou [a], Ping Shen [a], Zhongming Gao [b], Qichuan Jiang [a,*]

[a] *Key Laboratory of Automobile Materials of Ministry of Education, Department of Materials Science and Engineering, Jilin University, Changchun, Jilin 130025, PR China*
[b] *State Key Laboratory of Inorganic Synthesis & Preparative Chemistry, Jilin University, Changchun, Jilin 130012, PR China*

Received 5 November 2007; received in revised form 12 February 2008; accepted 29 February 2008
Available online 14 April 2008

Abstract

Self-propagating high-temperature synthesis (SHS) of compacted blends of Ti, B_4C and/or C powders was used to fabricate in situ TiC_x–TiB_2 composites with different compositions. The microstructures of the resultant products were studied by X-ray diffraction (XRD) and field emission scanning electron microscopy (FESEM), and the reaction sequence in the SHS reaction process was explored by quenching the combustion wavefront. The results showed that the TiC_x–TiB_2 composites with 27.4, 36.7 and 61.7% TiB_2 in molar fractions display hypoeutectic, eutectic and hypereutectic microstructures, respectively, and TiC_x is the leading phase in formation of the eutectic phase during solidification. Moreover, substoichiometric TiC_x forms prior to TiB_2 in phase formation sequence even for the hypereutectic composition sample.

Keywords: Self-propagating high-temperature synthesis (SHS); Composites; Microstructure-final; TiC; TiB_2

1. Introduction

TiC–TiB_2 composites possess not only high-melting points, high hardness, excellent wear resistance and good thermal stability, but also superior properties such as enhanced fracture toughness and bending strength compared with constituent ceramic components.[1,2] Therefore, TiC–TiB_2 ceramic composites are attractive for application as advanced structural materials, and many methods, such as reactive sintering,[3] reaction hot pressing,[4] spark plasma synthesis,[5] transient plastic phase processing,[6] and self-propagating high-temperature synthesis (SHS), also termed combustion synthesis (CS)[2,7] have been developed for the synthesis of such TiC–TiB_2 ceramic composites.

On the other hand, TiC_x–TiB_2 has been demonstrated to be a eutectic system[8–12] and the eutectic composition and temperature of this system are significantly dependent on the composition of TiC_x.[8,11] According to the Ti–C phase diagram,[13] the value of x in TiC_x ranges from 0.47 to 1.0 and the eutectic point of the TiC_x–TiB_2 system, as indicated in Fig. 1, may shift from e_1 to e_2 as the value of x varies from 0.47 to 1.0. The eutectic points given in Fig. 1 might not be accurate since considerable controversy exists in the reported eutectic composition and temperature for the TiC_x–TiB_2 system in the past years. Some representative values obtained by both experimental measurement and theoretical calculation are shown in Table 1. One possible reason for the large scatter might be the influence of the variable composition of TiC_x with its range of stoichiometry, especially on the eutectic temperature. Another is that it might be rather difficult to accurately determine the eutectic composition in the TiC_x–TiB_2 system regarding the difficulty in measuring the compositions of the light elements (boron and carbon). Therefore, more delicate and powerful measurements need to be carried out in order to clarify this confusion.

In this study, we prepared TiC_x–TiB_2 composites with different compositions using Ti–B_4C and Ti–B_4C–C systems by SHS and examined their microstructures, from which the eutectic composition for the TiC_x–TiB_2 system was suggested. It is worth mentioning that Zhang et al.[2] and Song et al.[7] also fabricated TiC–TiB_2 composites with different compositions by SHS using proper proportions of Ti, B_4C and C powders. However, the relationship between the composition of the products and

* Corresponding author. Tel.: +86 431 8509 4699; fax: +86 431 8509 4699.
E-mail address: jqc@jlu.edu.cn (Q. Jiang).

0955-2219/$ – see front matter © 2008 Elsevier Ltd. All rights reserved.
doi:10.1016/j.jeurceramsoc.2008.02.014

Table 1
The reported eutectic composition and temperature in the TiC_x–TiB_2 system[8–12]

Reaction	Eutectic composition (mol.% TiB_2)	Eutectic temperature (°C)	Method	Reference
$L \leftrightarrow TiC_{0.92} + TiB_2$	43	2620	Experiment	[8]
$L \leftrightarrow TiC_{0.95} + TiB_2$	44	2520	Experiment	[9]
$L \leftrightarrow TiC_{0.68} + TiB_2$	–	2380	Experiment	[9]
$L \leftrightarrow TiC_{0.92} + TiB_2$	35	2600	Experiment	[10]
$L \leftrightarrow TiC_{0.6} + TiB_2$	40.1	2637	Calculation	[11]
$L \leftrightarrow TiC_{0.8} + TiB_2$	40.5	2688	Calculation	[11]
$L \leftrightarrow TiC_{1.0} + TiB_2$	40.2	2663	Calculation	[11]
$L \leftrightarrow TiC + TiB_2$	28	–	Experiment	[12]

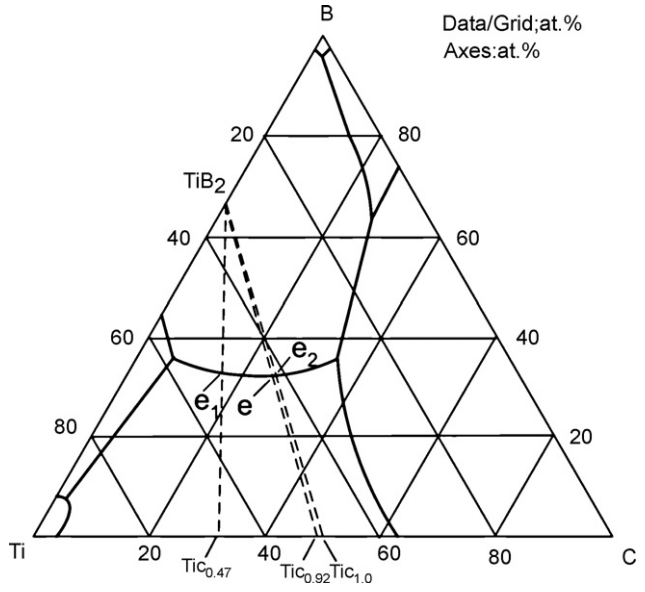

Fig. 1. A schematic projection of liquidus surface of the Ti–B–C ternary phase diagram (after Rudy and Windisch[8]).

their microstructures was not reported therein. Also, the formation mechanism of TiC_x and TiB_2 in the SHS reaction was proposed in the present paper. Such understandings are expected to promote the development of the TiC_x–TiB_2 composites with tailored microstructures.

2. Experimental procedure

The characteristics of the starting powders with their sources are presented in Table 2. The theoretical molar ratios of TiC:TiB_2 in the products were predetermined to be 2.33:1, 1.47:1 and 1:2, based on the following reactions:

$$3.33Ti + 0.5B_4C + 1.83C \rightarrow 2.33TiC + TiB_2 \quad (1)$$

$$2.47Ti + 0.5B_4C + 0.97C \rightarrow 1.47TiC + TiB_2 \quad (2)$$

$$3Ti + B_4C \rightarrow TiC + 2TiB_2 \quad (3)$$

Powder blends with proper proportions were dry-mixed in a stainless-steel container using stainless-steel balls at a low speed (~35 rpm) for 8 h to ensure homogeneity. The mixtures were uniaxially pressed into cylindrical compacts of 22 mm in diameter and 15 mm in height at pressure ~60 MPa with green densities of 65 ± 2% of theoretical, as determined from weight and geometric measurements.

The SHS experiments were conducted in a self-made stainless-steel vessel. The compact was placed on a graphite-flat with a thickness of ~2 mm, below which a tungsten electrode was set up as the reaction ignition source. The vessel was first evacuated and then filled with industrial argon (99.9%) at 1 atm. The reaction was initiated by arc heating, which was generated by passing a strong current between the tungsten electrode and the graphite-flat. As soon as the SHS reaction was initiated, the power was switched off. Phase analysis and microstructure of

Table 2
The characteristics of the powder reactants used in this study

Reactant	Source	Purity (wt.%)	Particle size (μm)
Ti	Institute of Nonferrous Metals, Pekin, China	99.5	~50
B_4C	Abrasive Ltd. Co., Dunhua, China	≥95[a]	~3.5
Graphite	Graphite Ltd. Co., Jilin, China	99.5	~1

[a] The main impurities are dissociative boron and carbon together with <1 wt.% Fe_2O_3.

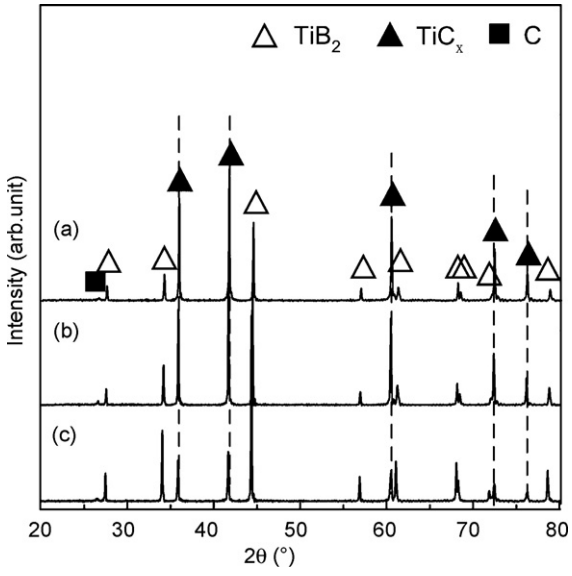

Fig. 2. XRD patterns of the SHS reaction products with (a) 27.4 mol.% TiB_2, (b) 36.7 mol.% TiB_2 and (c) 61.7 mol.% TiB_2, respectively.

the SHS products were investigated by X-ray diffraction (XRD) (D/Max 2500PC Rigaku, Tokyo, Japan) using Cu Kα radiation and field emission scanning electron microscopy (FESEM, JSM 6700F, Tokyo, Japan). In order to eliminate residual stress in the SHS products, which could have an effect on the lattice parameter calculation for the synthesized TiC_x, the samples were crushed into fine powders for XRD examination. In order to further release the residual stress, the powders were annealed at 600 °C for 2 h in a vacuum (5×10^{-3} Pa) furnace with heating and cooling rates of 20 °C/min and then reexamined by XRD.

In order to make clear the phase formation sequence in the SHS process, it was necessary to quench the combustion wave during its passage through the sample. Considerable efforts were then made for an automatic arresting of the combustion wave and success was achieved by using coarse B_4C powder (20–28 μm) and a rectangular bar in dimensions of 65 mm × 10 mm × 2 mm with a relative green density of ∼65 ± 2%. Both the coarse B_4C particle and the long and thin shape of the rectangular bar favor the extinction of combustion at the halfway point by reducing heat production and increasing heat loss. The phases in the different regions of the quenched sample were identified by X-ray micro-diffraction (D8 Discover with GADDS, Bruker AXS, Karlsruhe, Germany).

3. Results and discussion

Fig. 2 shows the XRD patterns for the product powders before annealing. The products consist of TiC_x, TiB_2 and a trace of carbon in all the samples. The reason why carbon remains is ascribed to the substoichiometry of the TiC_x phase, making carbon overabundant. During the SHS process, the reaction time is short (ranging between several seconds to several tens of seconds for temperature higher than 727 °C) and cooling rate is rapid (of the order of $10–10^2$ °C/s) so that it was generally incomplete for the stoichiometric TiC to develop. The stoichiometry of the TiC_x phase was estimated to be 0.77 ± 0.02 before the annealing treatment and to be 0.74 ± 0.02 after the annealing treatment based on the available relationship between the

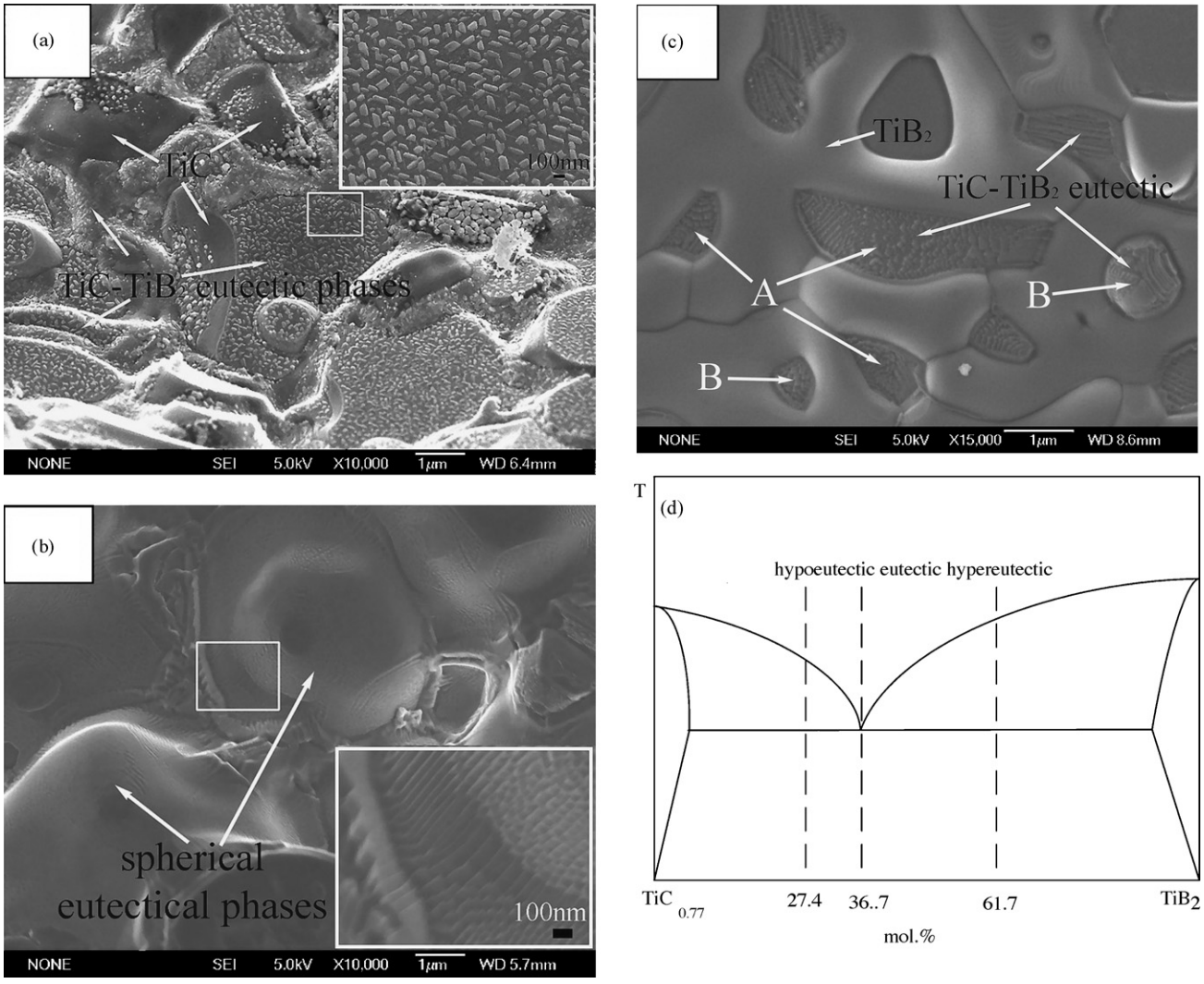

Fig. 3. FESEM micrographs of the fractured surfaces for the samples with (a) 27.4 mol.% TiB_2, (b) 36.7 mol.% TiB_2 and (c) 61.7 mol.% TiB_2 in the products showing (a) hypoeutectic, (b) eutectic and (c) hypereutectic microstructures (A-repulsed eutectic and B-engulfed eutectic), respectively, and (d) the schematic quasi-binary $TiC_{0.77}$–TiB_2 phase diagram without consideration of temperature.

lattice parameter of TiC_x and its stoichiometry,[13] and it does not seem to vary significantly with the carbon content in the reactants. The elimination of the residual stress by annealing does not seem to exert a significant effect on the TiC_x lattice parameter. Based on the quantitative calculations using the XRD results (Fig. 2), the volume fractions of TiB_2 in the synthesized composites were approximately 32.4, 42.3 and 67.1%, respectively, without taking the remnant carbon into account. Assuming that the theoretical densities of TiC and TiB_2 are 4.92×10^3 kg m^{-3} and 4.53×10^3 kg m^{-3},[14] the molar fractions of TiB_2 in the synthesized composites are 27.4, 36.7 and 61.7%, respectively.

Fig. 3(a–c) shows the typical microstructures of the fractured surfaces of the synthesized samples. As indicated in Fig. 3(a), the agglomerated phases with spherical or irregular shapes are primary TiC_x and the TiC_x–TiB_2 eutectic phases are observed among the primary TiC_x, which implies that during the solidification process, the redistribution of the boron solute in the melt proceeds as the crystallization of the primary TiC_x phase occurs, and the eutectic melt among the primary TiC_x particles solidifies in the end. The fine granular phase (see more clearly in the embedded enlarged graph) in the eutectic phases is TiB_2. The entire structure corresponds to a hypoeutectic one if the schematic quasi-binary phase diagram of $TiC_{0.77}$–TiB_2 [see Fig. 3(d)] is followed. In Fig. 3(b), a fine laminar eutectic structure (see the embedded enlarged graph) is widely observed in the spherical phases, suggesting that the eutectic reaction of liquid $\rightarrow TiC_x + TiB_2$ proceeds extensively during the solidification process. The width of the eutectic stripes obtained by the SHS reaction is ~100 nm. Repeated experiments gave the similar compositions and microstructures, implying that the eutectic composition in the $TiC_{0.77}$–TiB_2 system is around 36.7 mol.% TiB_2, as inferred from the quantitative XRD results. This result is in general agreement with the compositions experimentally determined by Beratan[10] and theoretically calculated by Gusev,[11] as presented in Table 1, but is somewhat different from the compositions measured by Rudy and Windisch[8] and Ordanyan et al.[9] Moreover, the eutectic composition of 28 mol.% TiB_2 measured by Li et al.[12] obviously conflicts with the above results. Fig. 3(c) shows a hypereutectic structure for the $TiC_{0.77}$–TiB_2 system with a composition of 61.7 mol.% TiB_2, in which the net-shaped skeleton phase is TiB_2 and the surrounded fine granular or laminar phases are the TiC_x–TiB_2 eutectics. It is worth noting that most TiC_x–TiB_2 eutectics are distributed at the grain boundaries of the primary TiB_2 phase (as indicated by arrows A), even though some are engulfed (as indicated by arrows B), which implies that the carbon solute in the melt redistributes and its concentration increases with the progress of the solidification, and finally the eutectic melt solidifies.

The eutectic temperature was not determined in this study, but the adiabatic combustion temperatures (T_{ad}) for reactions (1)–(3) were calculated to be 2920 °C (i.e., the melting point of TiB_2. It is worthwhile to mention that although the T_{ad} values are the same for reactions (1)–(3), the melting fraction of TiB_2 in the products is quite different) using thermodynamic data[15] based on the assumptions of the SHS reaction initiating at 25 °C and

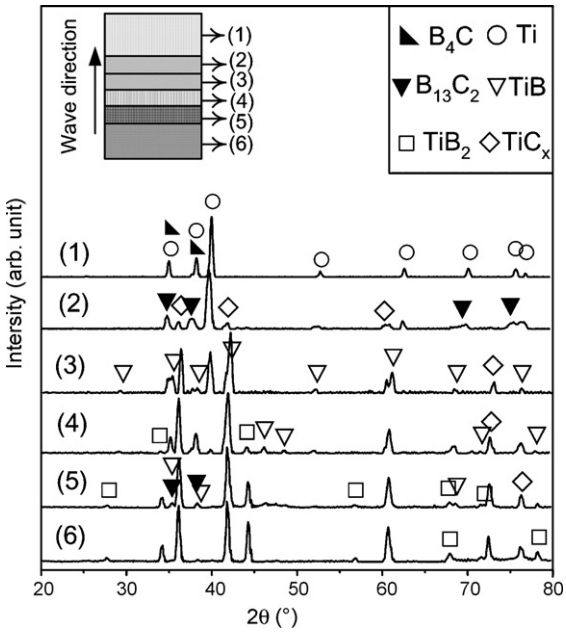

Fig. 4. X-ray micro-diffraction patterns for the quenched 3Ti–B_4C sample in the different regions: (1) green reactant region, (2) preheated region, (3) between the preheated region and combustion region, (4) combustion region, (5) post-combustion region and (6) product region.

no eutectic transformation between TiC_x and TiB_2. The reported eutectic temperatures, as shown in Table 1, are generally in the range of 2380–2688 °C. In this sense, the eutectic transformation was quite possible for the synthesized products to experience during the solidification process.

In order to investigate the phase formation sequence in the SHS reaction, quenching the combustion front of the 3Ti–B_4C sample was carried out. Fig. 4 shows the X-ray micro-diffraction patterns for the quenched sample in the different regions. As indicated, the phase transformation sequence could be described as

$$\begin{aligned} Ti + B_4C &\rightarrow Ti + B_{13}C_2 + TiC_x \\ &\rightarrow Ti + B_{13}C_2 + TiC_x + TiB \\ &\rightarrow Ti + B_{13}C_2 + TiC_x + TiB + TiB_2 \\ &\rightarrow B_{13}C_2 + TiC_x + TiB + TiB_2 \rightarrow TiC_x + TiB_2 \end{aligned}$$

Therefore, the SHS reaction path for the Ti–B_4C system might be as follows:

$$Ti + B_4C \rightarrow B_{13}C_2 + TiC_x \quad (4)$$

$$Ti + B_{13}C_2 \rightarrow TiC_x + TiB \quad (5)$$

$$TiB + B_{13}C_2 \rightarrow TiC_x + TiB_2 \quad (6)$$

Zhao and Cheng[3] investigated the reaction path for the 3Ti–B_4C sample during the reactive sintering process and proposed that the reaction path at high temperatures ($T > 1320$ °C) was

$$5Ti + B_4C \rightarrow TiC + 4TiB \quad (7)$$

$$6TiB + B_4C \rightarrow TiC + 5TiB_2 \quad (8)$$

In comparison, the difference lies in that boron-rich carbide ($B_{13}C_2$) substituted for B_4C and nonstoichiometric TiC_x forms prior to TiB. The reasons have been detailedly described in our previous paper,[16] and could be attributed to the fact of much faster dissociation and diffusion rates of carbon from the B_4C crystal than those of boron. As for the Ti–B_4C–C system, although the quenching of the combustion front was not carried out, the reaction:

$$Ti + C \rightarrow TiC_x \quad (9)$$

could be the first step in the SHS reaction, and a similar conclusion has been drawn by Locci et al.[5] in their spark plasma synthesis reaction study.

It should be pointed out that although TiC_x forms prior to titanium boride in the phase formation sequence, the TiC_x precursor is highly substoichiometric in nature. According to the Ti–C phase diagram,[13] the melting point of TiC_x is dependent on its stoichiometry. For example, when $x = 0.47$, the melting point is approximately 1645 °C, and when $x = 0.75$, it increases to approximately 3070 °C. Therefore, the TiC_x precursor will dissolve back into the titanium melt with the increase in temperature as the SHS reaction progresses (namely, the highly substoichiometric TiC_x precursor could be retained only when the reaction is quenched, as shown in Fig. 4). During solidification, TiC_x nucleates preferentially in the hypoeutectic 27.4 mol.% TiB_2 sample and so does TiB_2 in the hypereutectic 61.7 mol.% TiB_2 sample. They are primary TiC_x and TiB_2 phases, respectively, as shown in Fig. 3(a) and (c). When the composition moves to the eutectic point or alternatively, for the eutectic composition sample, the leading phase in the eutectic transformation is TiC_x rather than TiB_2. This can be inferred from the spherical morphology of the eutectic phases as shown in Fig. 3(b), which is similar to the typical shape of TiC_x in the combustion-synthesized samples.[17] On the other hand, the concentration condition for TiC_x nucleation is easier to be satisfied as compared with that of TiB_2 because of the substoichiometry nature of TiC_x and the much faster diffusion rate of carbon in titanium than that of boron.[6,16]

4. Conclusions

The TiC_x–TiB_2 composites with the hypoeutectic, eutectic and hypereutectic microstructures have been successfully fabricated using titanium, boron carbide and graphite reactants by the SHS reactions. The eutectic composition for the $TiC_{0.77}$–TiB_2 system was around 63.3 mol.% TiC–36.7 mol.% TiB_2, and TiC_x is the leading phase for the formation of the eutectic. The reaction path in the Ti–B_4C–C samples during the SHS process was (i) $Ti + C \rightarrow TiC_x$, (ii) $Ti + B_4C \rightarrow B_{13}C_2 + TiC_x$, (iii) $Ti + B_{13}C_2 \rightarrow TiC_x + TiB$, and (iv) $TiB + B_{13}C_2 \rightarrow TiC_x + TiB_2$.

Acknowledgements

This work is supported by the National Natural Science Foundation of China (No. 50531030), the National 863 project of China (No. 2006AA03Z566) and the Ministry of Science and Technology of China (No. 2005CCA00300) as well as by the 985 Project-Automotive Engineering of Jilin University.

References

1. Levine, S. R., Opila, E. J., Halbig, M. C., Kiser, J. D., Singh, M. and Salem, J. A., Evaluation of ultra-high temperature ceramics for aeropropulsion use. *J. Eur. Ceram. Soc.*, 2002, **22**, 2757–2767.
2. Zhang, X. H., Zhu, C. C., Qu, W., Zhang, X. D. and Kvanin, V. L., Self-propagating high temperature combustion synthesis of TiC/TiB_2 ceramic–matrix composites. *Comp. Sci. Technol.*, 2002, **62**, 2037–2041.
3. Zhao, H. and Cheng, Y. B., Formation of TiB_2–TiC composites by reactive sintering. *Ceram. Int.*, 1999, **25**, 353–358.
4. Gotman, I., Travitzky, N. A. and Gutmanas, E. Y., Dense in situ TiB_2/TiN and TiB_2/TiC ceramic matrix composites: reactive synthesis and properties. *Mater. Sci. Eng. A*, 1998, **244**, 127–137.
5. Locci, A. M., orrù, R., Cao, G. and Munir, Z. A., Simultaneous spark plasma synthesis and densification of TiC–TiB_2 composites. *J. Am. Ceram. Soc.*, 2006, **89**, 848–855.
6. Brodkin, D., Kalidindi, S. R., Barsoum, M. W. and Zavaliangos, A., Microstructural evolution during transient plastic processing of titanium carbide–titanium boride composites. *J. Am. Ceram. Soc.*, 1996, **79**, 1945–1952.
7. Song, I., Wang, L., Wixom, M. and Thompson, L. T., Self-propagating high temperature synthesis and dynamic compaction of titanium diboride/titanium carbide composites. *J. Mater. Sci.*, 2000, **35**, 2611–2617.
8. Rudy, E. and Windisch, S., Ternary phase equilibria in transition metal–boron–carbon–silicon systems. Part II. Ternary systems. *Phase Diagrams of the Systems Ti–B–C, Zr–B–C and Hf–B–C, vol. XIII*, Report No. AFML-TR-65-2, Contract No. USAF 33(615)-1249, Air Force Materials Laboratory, Wright-Patterson Air Force Base, Ohio, 1966, pp. 1–212.
9. Ordanyan, S. S., Unrod, V. I. and Avgustinik, A. I., Reactions in the system TiC_x–TiB_2. *Powder Metall. Met. Ceram.*, 1975, **14**, 729–731.
10. Beratan, H.R., *The Directional Solidification and Properties of the TiC–TiB_2 Eutectic*, M.S. thesis. Pennsylvania State University, Philadelphia, PA, 1980.
11. Gusev, A. I., Phase equilibria in the ternary system titanium-boron-carbon: the sections TiC_y–TiB_2 and B_4C_y–TiB_2. *J. Solid State Chem.*, 1997, **133**, 205–210.
12. Li, W. G., Tu, R. and Goto, T., Preparation of direction solidified TiB_2–TiC eutectic composites by a floating zone method. *Mater. Lett.*, 2006, **60**, 839–843.
13. Holt, J. B. and Munir, Z. A., Combustion synthesis of titanium carbide: theory and experiment. *J. Mater. Sci.*, 1986, **21**, 251–259.
14. Samsonov, G. V. and Vinitskii, I. M., *Handbook of refractory compounds*. IFI/Plenum Publishing Corporation, NY, 1980.
15. Barin, I., *Thermochemical data of pure substances* (*3rd ed.*). Wiley-VCH Verlag GmbH, Germany, 1995.
16. Shen, P., Zou, B. L., Jin, S. B. and Jiang, Q. C., Reaction mechanism in self-propagating high temperature synthesis of TiC–TiB_2/Al composites from an Al–Ti–B_4C system. *Mater. Sci. Eng. A*, 2007, **454/455**, 300–309.
17. Jiang, Q. C., Li, X. L. and Wang, H. Y., Fabrication of TiC particulate reinforced magnesium matrix composites. *Scripta Mater.*, 2003, **48**, 713–717.